atoms

IMPACT FACTOR 1.8

CITESCORE 3.1

Review

Progress in High-Precision Mass Measurements of Light Ions

Edmund G. Myers

MDPI

https://doi.org/10.3390/atoms12020008

atoms

MDPI

Review

Progress in High-Precision Mass Measurements of Light Ions

Edmund G. Myers

Department of Physics, Florida State University, Tallahassee, FL 32306-4350, USA; emyers@fsu.edu

Abstract: Significant advances in Penning trap measurements of atomic masses and mass ratios of the proton, deuteron, triton, helion, and alpha-particle have occurred in the last five years. These include a measurement of the mass of the deuteron against ^{12}C with 8.5×10^{-12} fractional uncertainty; resolution of vibrational levels of H_2^+ as mass and the application of a simultaneous measurement technique to the H_2^+/D^+ cyclotron frequency ratio, yielding a deuteron/proton mass ratio at 5×10^{-12}; new measurements of $HD^+/^3He^+$, HD^+/T^+, and $T^+/^3He^+$ leading to a tritium beta-decay Q-value with an uncertainty of 22 meV, and atomic masses of the helion and triton at 13×10^{-12}; and a new measurement of the mass of the alpha-particle against ^{12}C at 12×10^{-12}. Some of these results are in strong disagreement with previous values in the literature. Their impact in determining a precise proton/electron mass ratio and electron atomic mass from spectroscopy of the HD^+ molecular ion is also discussed.

Keywords: atomic mass; fundamental constants; precision measurement; Penning trap

1. Introduction

The atomic masses of the proton, deuteron, triton, helion, and alpha-particle (usually called the light ions) and their ratios enter into a broad range of physical science and so are considered to be fundamental physical constants. While for most of physics and chemistry, the values in the Committee on Data of the International Science Council (CODATA-2018) least squares adjustment [1] are more than sufficiently precise, there are applications where this is not the case. Specifically, improved mass ratios of the proton and deuteron to the electron are motivated by ongoing advances in the rotational and vibrational spectroscopy of diatomic molecular hydrogen ions; while improved masses of helium isotopes are required for measurements of g-factors (magnetic moments) of one-electron helium ions. Another important application is in the determination of absolute (anti)neutrino mass from tritium beta-decay, requiring a precise value for the mass difference between tritium and helium-3. From the purely metrological perspective, new measurements are also motivated by discrepancies involving previous measurements, as in the so-called "light-ion (or ^{3}He) mass puzzle" [2].

After more details on motivations, we give a brief review of techniques for precision Penning trap cyclotron frequency ratio (CFR) measurements as applied to light ions (Section 2), and of the measurements that have occurred since a previous review [3] (Section 3). We then discuss the results and their impact (Section 4), and finish with some indications for future work (Section 5).

When the distinction is important, we use M[x] for the mass of x expressed in u (1/12 the mass of an atom of ^{12}C), but otherwise we use m_x. We emphasize that it is only mass ratios, particularly relative to the electron, that are important for precision applications. For light ions and their molecular ions (and for carbon), it should be understood that any CFR can be converted into an equivalent mass ratio of any charge state of the respective isotopes (e.g., between their nuclei, or the neutral atoms). This is because the electron atomic mass and all the required binding energies are known to a more than adequate precision [1]. A precise mass ratio can also be converted to an equivalent mass difference without loss of precision. All uncertainties are one-standard deviation.

Citation: Myers, E.G. Progress in High-Precision Mass Measurements of Light Ions. *Atoms* **2024**, *12*, 8. https://doi.org/10.3390/atoms12020008

Academic Editor: Maxime Brodeur

Received: 20 December 2023
Revised: 18 January 2024
Accepted: 23 January 2024
Published: 26 January 2024

1.1. Spectroscopy of Molecular Hydrogen Ions

There has been considerable recent progress in the ab initio, quantum–electrodynamics (QED)-based theory of the rovibrational energies of diatomic molecular hydrogen ions, e.g., see [4–6]. While precision spectroscopy of two-photon and electric quadrupole transitions in H_2^+ and D_2^+ can be expected in the near future [7–9], all published measurements so far have been for HD^+ in which electric dipole transitions occur [10–13]. Since the theoretical predictions for HD^+ transitions depend on m_p/m_e and m_d/m_p (or m_d/m_e), these mass ratios, as obtained from Penning traps, are necessary for testing the HD^+ theory. The agreement between theory and experiment, within their combined uncertainties, can then be used to put limits on beyond-standard-model physics, such as a Yukawa-type Angstrom-range interaction between the nuclei [14]. Alternatively, the HD^+ spectroscopic results, combined with a Penning trap measurement of m_d/m_p, can be used to obtain m_p/m_e and hence $M[e]$.

1.2. Measurements of g-Factors to Obtain M[e]

The CODATA-2018 value for the electron atomic mass, with uncertainty of 2.9×10^{-11} [1], is obtained from the combination of QED theory [15,16] and experiment [17,18] for the g-factor (magnetic moment in units of the Bohr magneton) of hydrogen-like carbon. (To obtain a precise m_{ion}/m_e from a CFR measurement is difficult due to the electron's relativistic mass increase [19]; it may be possible using a Penning trap at milli-kelvin temperature [20]). The g-factor measurement consists of measuring, in the same magnetic field, the microwave frequency that induces a spin-flip of the electron in the ground state of the hydrogen-like ion, f_{sf}, and the ion's cyclotron frequency, f_c. (The spin-flip is detected using the "continuous Stern-Gerlach technique" [21]). In a magnetic field B, the electron spin-flip frequency is given by $f_{sf} = g_{ion}B\mu_B/h = (g_{ion}B/4\pi)(e/m_e)$, where g_{ion} is the g-factor and μ_B, h, e, m_e have their usual meanings. By measuring the ion's cyclotron frequency, $f_c = eB/(2\pi)m_{ion}$, the magnetic field can be cancelled to give $f_{sf}/f_c = (1/2)\, g_{ion}\, (m_{ion}/m_e)$. Hence, by measuring f_{sf}/f_c and making use of a theoretical value for g_{ion}, a value for (m_{ion}/m_e) can be obtained. This yields $M[e]$ provided $M[ion]$ is known to sufficient precision.

1.2.1. $^4He^+$

A future measurement of the g-factor of $^4He^+$ has advantages compared to $^{12}C^{5+}$ as a route to obtaining $M[e]$. First, because the difficult-to-calculate two-loop QED corrections and the nuclear size corrections scale rapidly with nuclear charge, the theoretical uncertainty for the g-factor of $^4He^+$, currently at 2.8×10^{-13}, is two orders of magnitude smaller than for $^{12}C^{5+}$ [15]. But, second, the measurements have the advantage of smaller image charge and relativistic corrections (see below). This motivates a precision measurement of M [^{4}He].

1.2.2. $^3He^+$

Measurements of the shielded nuclear g-factor, hyperfine structure, and electronic g-factor have recently been carried out in $^3He^+$ [22]. With application to absolute calibration of magnetic fields using the ^{3}He nuclear magnetic resonance (NMR) frequency, the helion nuclear g-factor was obtained with a relative precision of 8×10^{-10}. The electronic g-factor was measured to 2.3×10^{-10}. Although the electronic g-factor measurement is not competitive with $^{12}C^{5+}$, the experimental precision could be improved, motivating an improved M [^{3}He].

1.2.3. Molecular Hydrogen Ions

The continuous Stern–Gerlach technique can also be applied to electron-spin-state detection in molecular hydrogen ions, and hence to measuring electronic g-factors, hyperfine structure, and shielded g-factors of the proton (and anti-proton), deuteron, and triton [23]. An initial experiment on HD^+ has been completed [24], while measurements on H_2^+ and other isotopologues are planned. As for one-electron atomic ions, the measurements yield $g_{ion}(m_{ion}/m_e)$, although here the g-factors depend on the rovibrational state and also the

Zeeman sub-state. Although published theory for the electron g-factors has so far been developed only up to the lowest-order relativistic corrections [25], improvements could be made in the future. In this case, precise masses of hydrogen isotopes will be needed to test the theory.

1.3. Mass Difference between Tritium and Helium-3 for Neutrino Mass

Several large-scale studies of neutrino oscillations have confirmed that neutrinos created in weak interaction processes are superpositions of three mass eigenstates, and have produced increasingly accurate values for the mixing parameters and differences in the squares of the three masses [26]. However, they give no information on absolute neutrino mass, which is an outstanding question for both particle physics and cosmology. One of the most direct laboratory methods for determining absolute neutrino mass is the study of the beta-decay spectrum of tritium near the endpoint. The KATRIN tritium beta-decay experiment has already produced a limit on effective electron neutrino mass, $m(\nu_e) < 0.8$ eV$/c^2$, (90% CL), and aims to improve this to 0.2 eV$/c^2$ [27]. Currently under development, Project-8 uses the novel technique of cyclotron radiation emission spectroscopy [28] and has the goal of a limit on $m(\nu_e) < 0.04$ eV$/c^2$. In addition to limits on $m(\nu_e)$, which are obtained from values for $m(\nu_e)^2$, these experiments produce a value for E_0, the "endpoint for zero neutrino mass". E_0 can be directly related to the Q-value of tritium beta decay, which is directly related to the mass difference between atoms of tritium and helium-3. A precise value for M[T] $-$ M [^{3}He] checks the value for E_0 obtained in the beta-decay experiments. This tests the understanding of the energy loss processes in KATRIN and Project-8, hence validating the resulting limits on $m(\nu_e)$.

2. Methods for Atomic Mass Measurements on Light Ions

The current mass measurements of light ions at the highest precision all involve measuring CFRs of pairs of ions in cryogenic Penning traps [21,29,30]. The Penning trap consists of a set of electrodes producing a quadratic electrostatic potential, immersed in the uniform and stable field of a superconducting magnet. The electrostatic potential results in confinement of the ion along the direction of the magnetic field and a corresponding "axial" oscillation at frequency f_z, which is typically ~500 kHz. The quadratic potential slightly reduces the frequency of the cyclotron motion from that in the magnetic field alone, f_c, to the "trap-modified cyclotron frequency", f_{ct}. It also produces a second circular motion about the electrostatic center of the trap called the magnetron motion, which is at a frequency f_m, which is slightly above ${f_z}^2/2f_{ct}$ and is a few kHz. The motions of the ions are detected, and their frequencies measured, by detecting image currents induced between electrodes of the trap. A precise value for $f_c \equiv qB/(2\pi m)$, corresponding to the magnetic field without the electrostatic potential, is obtained using the "invariance theorem" ${f_c}^2 = {f_{ct}}^2 + {f_z}^2 + {f_m}^2$ [21]. This is exact in the limit of zero amplitudes of motion despite imperfections in the magnetic field and electrostatic potential. However, with such imperfections and due to special relativity, the three mode frequencies f_z, f_{ct}, and f_m are each functions of the amplitude of the axial motion a_z, and of the radii of the cyclotron and magnetron motions ρ_c, ρ_m. The most important magnetic field imperfections are the linear and quadratic gradients along the axis and are denoted by B_1 and B_2; while the most important imperfections to the electrostatic potential are the perturbations denoted by C_4 and C_6 [21,31]. Due to the extreme vacuum resulting from surrounding the Penning trap with surfaces at liquid-helium temperature, ion lifetimes against collisions with neutrals can be months or longer, enabling long measuring campaigns with a single ion pair.

Since the overall methods for Penning trap mass measurements have been described several times previously, e.g., [29,32], we focus on the developments of the last 5 years. In this period, there have been just two groups carrying out measurements on hydrogen and helium isotopes. These are a group at Florida State University (FSU), Tallahassee, and a group at the Max-Planck Institute for Nuclear Physics (MPIK), Heidelberg (with collaborators from J.-G. University, Mainz; GSI, Darmstadt; and RIKEN, Saitama). For

light ions, the MPIK group has developed the LIONTRAP apparatus [32], while the FSU group has further developed a Penning trap system that was operated at the Massachusetts Institute of Technology (MIT) prior to 2003, but with ions with higher mass-to-charge ratios. Although not further discussed here, methods closely related to LIONTRAP have been used by the BASE collaboration at CERN to compare the mass of the H^- ion to that of the antiproton, as a test of matter–antimatter symmetry [33].

Compared to the Penning trap mass measurements on low-charged heavy ions with m/q around 30 or higher, measurements on light ions have the advantage of a high cyclotron frequency which reduces the relative importance of trap electrostatic imperfections. On the other hand, due to their smaller mass, relativistic effects are more significant. We also note that FSU has in general measured CFRs that are m/q and m "doublets", which has the advantage of suppressing many systematic errors (and it is the mass ratios, including the ratio compared to the electron mass, that are important for most applications.) However, this generally requires the use of molecular ions, which introduces the complications of rovibrational energy and polarizability. MPIK has instead measured light ions against highly charged carbon ions, hence directly obtaining atomic masses in u. Although the chosen ion pairs were m/q doublets (except for the proton), they were not m or q doublets, so the control of some systematic uncertainties was more challenging.

2.1. FSU Trap

The FSU Penning trap [29] consists of a ring and two endcaps, both with hyperboloidal internal surfaces, with polar and equatorial diameters of 12 mm and 14 mm, respectively. The electrodes are made of OFHC copper and are coated with powdered graphite on the inside to reduce charge patches. The magnetic field, which was 8.53 T, was shimmed to high-uniformity using a scanning NMR probe before installing the Penning trap. The changes in B_1 and B_2 due to the trap electrodes themselves were compensated using nickel wires wound around the vacuum can enclosing the trap. C_4 can be nulled using a pair of compensation electrodes between the trap ring and end-caps. The main electrostatic imperfection is hence that characterized by C_6, which is typically 1.3×10^{-3}.

The trap has 0.5 mm diameter holes in the center of the upper and lower end-caps. Ions of hydrogen or helium isotopes are made directly in the trap by injecting a molecular or atomic beam of the appropriate gas through the hole in the upper end-cap as a few-ms pulse, simultaneously with a collinear, ~5 nA, 750 eV beam of electrons from a field-emission point (FEP), mounted below the hole in the lower end-cap. In order to minimize the amount of gas entering the trap, the molecular beam is produced in a 1 m long, cryogenically pumped "injector cryostat", mounted above the original Penning trap system. After the requisite ion or ions are made in the trap, the injector is valved-off from the vacuum space containing the trap and allowed to warm up.

The axial motion of the ion is detected, and also damped, via the image currents it induces in a superconducting coil connected between ground and the upper end-cap. The coil is made of pure niobium and is located 1 m above the trap and outside the strong field region. Together with the capacitance of the trap electrodes and stray capacitance, the circuit acts as an LCR resonant circuit, with a resonance frequency of 688 kHz and a Q-factor of 34,000. The coil is inductively coupled to a dc-SQUID which acts as a pre-amplifier. The ion's cyclotron and magnetron motions are addressed by coupling them to the axial motion using tilted quadrupolar oscillatory electric drives at $f_{ct} - f_z$ and $f_z + f_m$, respectively [34].

The cyclotron frequency is measured using the "Pulse-and-Phase" (PnP) technique [35]. This proceeds by first cooling all three modes of the ion, then applying a few ms oscillatory voltage pulse near f_{ct} to one half of one of the compensation electrodes, to drive the cyclotron motion to a radius of typically 20 μm. The cyclotron motion is then allowed to evolve, unperturbed, for an evolution period T_{evol} up to 15 s (for light ions). A pulse at $f_{ct} - f_z$ is then applied which couples the cyclotron motion to the axial motion. By applying this coupling pulse with the appropriate product of amplitude and duration, i.e., as a (classical) "pi-pulse", the cyclotron motion is effectively converted to axial motion,

with the final phase of the cyclotron motion, ϕ, coherently mapped onto the axial motion. The axial motion is then read out using the axial detector. By repeating the PnPs with different T_{evol}, f_{ct} can be obtained from $f_{ct} = (1/2\pi)d\phi/dT_{evol}$. Provided the intrinsic noise from the SQUID is small compared to the thermal noise from the detection circuit, it can be shown that both the signal power, and the noise power in a given bandwidth, fall by similar factors as a function of detuning from the coil resonance. Hence, since a narrower axial frequency signal is advantageous for determining ϕ and f_z, the PnPs are typically carried out with f_z detuned from the coil resonance by four or five coil resonance widths, with sampling times of 4 or 8 s.

Since a major contribution to uncertainty in a CFR is the variation in the magnetic field between measurements of f_c on the two ions, it is essential to interchange the ions as rapidly as possible. With the FSU trap, most measurements have used a technique in which the two ions are simultaneously trapped, but alternated between the center of the trap and a large radius (usually 2 mm) "parking" cyclotron orbit [36]. The outer ion is re-centered using cyclotron-to-axial coupling with the axial motion damped by interaction with the detector resonance. The inner ion is swept out using a down-chirped cyclotron drive. In the re-centering process, which typically takes 5 min, the frequency synthesizer supplying the cyclotron-to-axial coupling drive, and the ring and compensation voltages, are adjusted in steps. This is to keep the drive close to $f_{ct} - f_z$ (f_{ct} and f_z change due to special relativity and trap imperfections as ρ_c decreases), and f_z relatively independent of a_z and close to the detector resonance. In the sweep-out, which usually takes 10 s, the phase of the cyclotron motion follows the phase of the cyclotron drive. Hence, the cyclotron radius can be precisely set by matching the cyclotron drive frequency at the end of the sweep to the relativistically down-shifted f_{ct} corresponding to the desired ρ_c.

With an ion in a large cyclotron orbit, its lifetime was found to be essentially indefinite, while at the center of the trap it varied between months and a few days, depending on the length of time (weeks, months) since the last cool-down of the apparatus. Presumably, the lifetime of a centered ion is reduced due to the direct line of sight to room temperature through the 0.5 mm hole in the upper end-cap.

2.2. LIONTRAP

The "Light Ion Trap" (LIONTRAP), located at the J.-G. Universität, Mainz has been described in detail in [32]. In contrast to the single FSU trap, LIONTRAP consists of five inter-connected Penning traps, made up of a tower of 38 cylindrical electrodes [37] in a 3.8 T magnetic field. The five traps are a "creation" trap, a "reference" trap, two "storage" traps, and a "measurement" (or "precision") trap. The measurements of CFRs use the measurement trap and the two storage traps, which are above and below the measurement trap. The trap tower is completely enclosed in its vacuum chamber, so protons and highly charged ions of C and O were produced inside the creation trap, using a target made of carbon-fiber-loaded polyether ether ketone (PEEK, $C_{19}H_{14}O_3$). The electron beam from the FEP initially passes through a hole in the target, but, after multiple reflections, expands due to space charge and hits the edges. Ablated atoms and molecules are then ionized and trapped. Trapped low-charged ions can then be multiply ionized to make highly charged ions.

The measurement trap has an internal diameter of 10 mm and a seven electrode design which, in principle, allows for the compensation of electrostatic anharmonicities up to C_{10}. This trap has a split central ring and split inner compensation electrodes for applying the cyclotron drives and quadrupole cyclotron–axial coupling, and also for detecting and cooling the cyclotron motion. Furthermore, (at least as used in the proton measurement discussed in [32]), it has four, high-quality-factor (Q) LCR-circuit image-current detectors, two for the axial and two for the cyclotron motions. These use coils wound from niobium–titanium (a type II superconductor) and transistor amplifiers, and are located in the strong magnetic field region. The doubling of detectors for each mode enables ions that are not m/q doublets to be brought to resonance with their corresponding detectors, at the same trap voltage and same magnetic field. This was especially important for the measurement

of the CFR of the proton to $^{12}C^{6+}$. In order to reduce the effects of magnetic field variation, the two ions in the pair whose CFR was to be measured were created and trapped, but with one ion in the measurement trap and the other in one of the storage traps. The ions were then shuttled, alternately, between the measurement trap and a storage trap; the interchange taking about 80 s.

The cyclotron frequency of an ion in the measurement trap was measured most precisely using the "Pulse-and-Amplify" (PnA) method [38]. The PnA is similar to the PnP method, but instead of applying the cyclotron-to-axial coupling as a pi-pulse at $f_{ct} - f_z$, which effectively converts the cyclotron motion to axial motion, the coupling pulse is applied at $f_{ct} + f_z$. This results in the phase-coherent parametric amplification of both the cyclotron and axial modes. Compared to the PnP method, this has the advantage of producing a final axial amplitude that is large enough for the phase measurement from a smaller initial cyclotron radius. This reduces amplitude-dependent systematic errors such as that due to special relativity. A disadvantage, unless B_2 and C_4 are small, is that the large cyclotron radius after the PnA results in a shift to f_z, so it must be measured independently. This was performed using the "dip technique", in which the spectrum of noise from the axial detector was recorded over several minutes with the ion near resonance. The ion's axial motion "shorts-out" the detector noise resulting in a dip in the noise at f_z [21].

3. Measurements

3.1. FSU Measurement of H_2^+/D^+ by Alternating between Large and Small Cyclotron Orbits [39]

With the aim of obtaining an improved result for m_d/m_p, the CFR of H_2^+ to D^+ was measured at FSU by simultaneously trapping a D^+ and H_2^+ and alternating them between the trap center and a 2 mm radius parking orbit [39]. The D^+ was produced by injecting CD_4 while the H_2^+ was produced by simply operating the FEP for a few seconds, which presumably desorbed H_2 from either the FEP itself or the holes in the endcaps. Because H_2 and H_2^+ have different internuclear separations, H_2^+ produced by ionization of H_2 can be produced in any of the bound vibrational levels up to $v = 19$ [40]. The vibrationally excited levels are all highly metastable, with lifetimes against spontaneous decay, which occurs primarily by electric quadrupole transitions, between 7 days (for more excited levels) to 22 days (for $v = 1$), [41] (see Table I of [39]). The extra mass-energy due to the rovibrational energy is significant. For instance, the energy difference between $v = 0$ and $v = 1$ increases the H_2^+ mass by approximately 1.4×10^{-10}. In a run of 7 h, 15 alternate measurements of f_c for each ion were obtained, resulting in a statistical precision per run for the $H_2^+(v,N)/D^+$ CFR as low as 4×10^{-11}. Hence, different vibrational levels of H_2^+ were partially resolved by their difference in f_c. This was the first mass spectroscopy of molecular vibrational energy.

Since the CFR resolution was not sufficient to determine the H_2^+ vibrational state in all runs, Stark quenching was used to increase the rate of rovibrational decay rate to the ground state [42]. In the large cyclotron orbit, the H_2^+ ion experiences a $v \times B$ motional electric field. This electric field mixes the ground and excited electronic states. This results in a small electric dipole moment which increases the rate of rovibrational decay. For $\rho_c = 2$ mm and $B = 8.5$ T, the lifetime of $v = 1$ is reduced to 2.13 days, while the lifetimes of higher excited levels are reduced to a few hours. In this way, simply by placing the H_2^+ in a 2 mm-radius cyclotron orbit for ~1 week, it was possible to measure the CFR with 7 H_2^+ ions that were almost certainly in the vibrational ground state. However, since the spacing between rotational energy levels was less than the CFR resolution, e.g., the spacing between $N = 0$ and $N = 2$ changes the CFR by only 11.5×10^{-12}, and because, even with Stark quenching, the mean lifetimes of the rotational levels are months or years, it was not possible to directly determine the H_2^+ rotational state. Hence, estimates of the shift and uncertainty in the final CFR due to the rotational energy of the seven H_2^+ ions were made by assuming a Boltzmann rotational distribution for the parent H_2, and then modeling the rovibrational cascade to the ground vibrational level. The resulting shift agreed with an estimate based on the spread of the measured CFRs. Including a contribution to allow for

the possibility that collisions with neutrals might also change the rotational level, the overall correction applied to the H_2^+/D^+ CFR due to H_2^+ rotational energy was 16(16) $\times 10^{-12}$.

The largest systematic correction and second largest uncertainty to the CFR was from the imbalance in the cyclotron radii used in the PnP measurements between H_2^+ and D^+, coupled with special relativity (SR). To obtain this shift and its uncertainty, ρ_c of both ions were systematically varied by varying the length of the cyclotron drive pulse T_d at a constant amplitude, and then extrapolating the plot of CFR against ${T_d}^2$ to zero. Except for a possible imbalance in the initial cyclotron energy, this extrapolation gives the CFR corrected for SR. The correction determined with this procedure was 41(7) $\times 10^{-12}$. A third significant systematic correction resulted from the fact that the f_c measurements of the H_2^+ and D^+ were carried out with the trap voltages set so that the H_2^+ and D^+ axial frequencies were, respectively, 80 Hz below and above the detector resonant frequency. This was done so that the change in trap voltage between the PNP measurements on the ions was reduced; hence, reducing the shift in the CFR due to the change in ion equilibrium position coupled with magnetic field gradient, i.e., the "$B_1 \Delta V$" shift. Since the ions were on different sides of the detector resonance, their measured axial frequencies were "pushed" in opposite directions due to the ion–detector interaction, which shifts the f_cs obtained using the invariance theorem. The required "coil-pushing" correction was 8.2(1.0) $\times 10^{-11}$. The remaining systematic shifts were the residual $B_1 \Delta V$ shift, needing a correction $-0.6(0.6) \times 10^{-12}$, and that due to the polarizability of the H_2^+ [43,44], needing a correction 1.1(0.3) $\times 10^{-12}$. The resulting total systematic correction was 65(18) $\times 10^{-12}$. With a statistical uncertainty of 6.3 $\times 10^{-12}$, the final result was $M[D^+]/M[H_2^+(0,0] = 0.999\,231\,660\,004(19)$.

3.2. MPIK Measurement of the Atomic Mass of the Deuteron and HD^+ [45]

Using the LIONTRAP apparatus previously used to measure the proton against $^{12}C^{6+}$ [32], the MPIK collaboration measured the CFR of the deuteron against $^{12}C^{6+}$ and of HD^+ against $^{12}C^{4+}$ [45]. Compared to the proton measurements, the quadratic magnetic field inhomogeneity was reduced from $B_2/B_0 = -7.2(4) \times 10^{-8}$ to 6.5(6.5) $\times 10^{-10}$ mm^{-2}. The stability of the magnetic field was also improved with the stabilization of the pressure of the liquid nitrogen and liquid helium reservoirs and by improved trap alignment. A single axial detector with resonance frequency near 461 kHz was used.

In order to load deuterons and HD^+ ions, a surface layer of a deuterated organic compound was printed onto the surface of the carbon-fiber-loaded PEEK target. Unlike the proton measurement, in both cases the ion pairs form a near m/q doublet, so the axial motion was detected using a single, tuned circuit. As for the proton measurement, the ions were shuttled into the measurement trap from the adjacent storage traps and measurements of f_c for each ion were obtained using the PnA method. Unlike the FSU procedure, where measurements were alternated between the ions, and a CFR measurement derived from a polynomial fit to both sets of f_c data for the entire run, in the LIONTRAP procedure a CFR measurement was considered to be the result of single measurements of f_c on each ion in the pair. The first ion was chosen at random, so successive measurements could be on the same ion. Each run typically produced 27 CFRs, which were then averaged to give a CFR for the whole run.

Over the $D^+/^{12}C^{6+}$ measurement campaign, 41 runs were obtained using 4 ion pairs, each trapped for 1 to 4 months. Analogous to the FSU H_2^+/D^+ measurements, to allow for amplitude dependent shifts due to SR, the cyclotron drive amplitudes A_i of both ions were varied, and an extrapolation made to zero ${A_i}^2$. Due to the lower magnetic field and the smaller minimum ρ_c of 10 microns in the PnA, the relativistic shifts were an order of magnitude smaller than for the FSU H_2^+/D^+ measurements. Feedback cooling was also used to reduce T_z to 1.2(5) K, which reduced the initial thermal ρ_c in the PnA. From the fit to the CFR data with different driven ρ_c, a $D^+/^{12}C^{6+}$ CFR with a statistical uncertainty of 5.4 $\times 10^{-12}$ was obtained.

Because the ions in each pair had a different mass, the initial thermal cyclotron energy did not cancel in the CFR, even if the ions had the same cyclotron temperature. This

required an SR correction of $-2.9(1.2) \times 10^{-12}$ to the $D^+/^{12}C^{6+}$ CFR. Overall, the largest systematic correction was due to the unequal image charges (again, resulting from the ions' different mass), $82.1(4.1) \times 10^{-12}$. However, the largest systematic uncertainty in the CFR overall, 4.7×10^{-12}, was in the determination of the axial frequency, which was performed with the dip technique. Since, on resonance with the detector, the FWHM of the dip due to the $^{12}C^{6+}$ was 3 Hz, determination of the ion's f_z to sufficient accuracy required a subdivision of the linewidth by a factor of 500. Due to the ion detector's pushing effect, the measured f_z was also sensitive to uncertainty in the detector resonance frequency. Because of the small B_2/B_0, the correction to the CFR for magnetic field imperfections was only $0.3(0.6) \times 10^{-12}$. Between measurements of f_c on each ion, the detector resonance frequency was shifted using a varactor, so the measurements were carried out at the same trap voltage, hence eliminating any $B_1 \Delta V$ shift. The combined systematic uncertainty was 6.5×10^{-12}, and the final value for the mass ratio $6M[D^+]/M\,[^{12}C^{6+}]$ was 1.007 052 737 911 7(85). This is the most precise result for a CFR directly relating to ^{12}C to date.

Similar techniques were used for the $HD^+/^{12}C^{4+}$ measurement. As in earlier work on HD^+ at FSU [2,46,47], due to its body-frame dipole moment the HD^+ was assumed to be in the rovibrational ground state, and a correction was made for its polarizability. From one ion pair trapped for 7 weeks $4M[HD^+]/M\,[^{12}C^{4+}]$ = 1.007 310 263 905(19)(8)(20) (stat)(sys)(total) was obtained.

3.3. FSU Measurement of H_2^+/D^+ Using Simultaneous Measurement of Cyclotron Frequencies in Coupled Magnetron Orbits [48]

In order to eliminate the uncertainty in a CFR measurement due to variation in the magnetic field, in the 1990s the MIT mass spectrometry group developed a technique in which the modified cyclotron frequencies of a pair of ions were measured simultaneously [49,50]. In this method, which is applicable to ion pairs with fractional mass difference in the range $10^{-4} < \Delta m/m < 10^{-3}$, the ions are placed in coupled magnetron orbits, such that the ions orbit the center of the trap, 180° apart, with nearly equal radii of ~0.5 mm. In this configuration, due to the Coulomb interaction between the ions, the magnetron modes of the ions are strongly coupled, while the axial and modified cyclotron modes, though perturbed, remain largely independent. Simultaneous PnP measurements can then be performed on the two ions. In 2002–2003, this technique was applied at MIT to ions with m/q near 30, producing four CFRs with the then world record uncertainties of 7×10^{-12}. After a 20-year hiatus, the method was re-developed at FSU and applied to a second measurement of the H_2^+/D^+ CFR, the first application to light ions.

More formally, the normal modes of the coupled magnetron motion are a "common-like mode", which approximates the motion of the center-of-charge of the ions, and a "separation-like mode", which approximates the vector difference between the ions. The ideal configuration corresponds to minimizing the amplitude of the common-like mode, while setting the amplitude of the separation-like mode, i.e., the ion–ion separation ρ_s, to its optimal value. As shown in [31], the CFR can then be derived from a precise value for the difference in the modified cyclotron frequencies of the two ions, $\Delta f_{ct} = f_{ct1} - f_{ct2}$, combined with less precise values of f_{ct1} and f_{z1} (or f_{ct2} and f_{z2}). The fractional uncertainties for f_{ct1} and f_{z1} can be larger than the fractional uncertainty in the CFR by factors of $m/\Delta m$ and $(f_{ct}/f_z)^2$ $(m/\Delta m)$, respectively. (A precise measurement of Δf_z is not required since the ions follow similar paths in the magnetic and electrostatic fields. Hence, effectively, Δf_z is determined by Δf_{ct}.) Applying the PNP technique simultaneously to both ions, the CFR measurement is essentially reduced to a precise measurement of the phase difference $\Delta\phi = 2\pi\Delta f_{ct} T_{evol}$, as determined from the phases of the simultaneous axial ring-down signals. Importantly, the sensitivity to shifts to f_z that would otherwise affect the CFR is greatly relaxed. Implementing this method required re-developing the important tool of "phase-locked driven axial motion" [31]. This allowed the continuous measurement of an ion's f_z in real time, and was essential for monitoring the amplitudes of the common and separation modes of the ion pair, and for cooling the common-mode motion.

A run began with (typically) a 15 min period of "phase-lock" cooling of any common-mode motion that had been produced in the previous run. The actual CFR measurement then consisted of cycles of simultaneous PnPs on the two ions, with a longest T_{evol} of 10.1 s, interleaved with PnPs with T_{evol} of 0.1, 0.3, 1.1, and 3.3 s, which were needed for phase unwrapping the individual f_{ct}. Throughout the run, phase coherence was maintained between all synthesizers used for the PnPs. Hence, the phases for different T_{evol} could be averaged over the whole run, and phase unwrapping applied to the averaged phases. After trials with different ion–ion separations it was found that ρ_s = 0.8 mm was optimum. This gave the best compromise between stability of the coupled magnetron motion, which improved with reduced ρ_s due to increased ion–ion coupling, and the need to minimize ion–ion induced axial anharmonicity, which could only be partially compensated by applying C_4.

The improvement in precision using the simultaneous technique was less dramatic than at MIT with m/q = 30. This was partly because the ambient magnetic field at FSU was more stable than at MIT, but also because, at low m/q, noise on f_{ct} due to fluctuations in ρ_c combined with SR was comparable in magnitude to noise due to magnetic field fluctuations. This SR noise on f_{ct} is given by $\sigma(f_{ct})/f_{ct} = (2\pi f_{ct}/c)^2\sigma(\rho_c{}^2)/2$, where $\sigma(\rho_c{}^2)$ is the rms fluctuation in $\rho_c{}^2$ from PnP to PnP. $\sigma(\rho_c{}^2)$ originates from the cyclotron motion at the start of the PnPs, which varies randomly from PnP to PnP, and which combines by phasor addition with the driven cyclotron motion, with the result $\sigma(\rho_c{}^2) = 2^{1/2}\rho_c{}^{th}\rho_c{}^{drive}$, where $\rho_c{}^{th}$ is the rms value of the initial cyclotron radius, and $\rho_c{}^{drive}$ is the radius produced by the drive (see Supplementary Materials of ref. [48]). $\rho_c{}^{th}$ is given by $\rho_c{}^{th} = (2k_BT_c/m)^{1/2}/(2\pi f_{ct})$, where T_c is the ion's effective cyclotron temperature resulting from cyclotron-to-axial coupling. In the ideal case, $T_c = (f_c/f_z)T_z$, where T_z is the ion's axial temperature. Hence, $\rho_c{}^{th}$, and the minimum $\rho_c{}^{drive}$ ($\sim 5\rho_c{}^{th}$) for adequate phase initialization in the PnP, are essentially independent of the ion's mass. So, overall, this relativistic noise varies as $f_{ct}{}^2$ and so is a more serious issue for light ions. In order to reduce this relativistic noise, T_z was reduced by a factor of 2 by applying electronic feedback to the axial motion of each ion, using the scheme described in [51]. This was executed with f_z shifted to resonance with the detector by changing the trap voltage. However, even with feedback, the overall gain in statistical precision in a 6 h run was only about a factor of two compared to a run with the alternating technique.

With ρ_s = 0.8 mm, both ions were outside the axial line of sight to room temperature. Further, the ions were not in large cyclotron orbits during the measurement. Hence, the average ion lifetime against collision with neutrals was considerably longer than with the alternating technique and excited vibrational levels did not undergo Stark quenching. Combined with the factor-of-two improved resolution, this enabled the tracking of the rovibrational decay of three different $H_2{}^+$ ions to the vibrational ground state. The rovibrational decays manifested as discrete jumps in the $H_2{}^+/D^+$ CFR between plateaus corresponding to a given rovibrational state. In one case, an $H_2{}^+$ was tracked from v = 9 to v = 0 over a period of more than two months. Taking account of the electric quadrupole selection rule for $H_2{}^+$ rovibrational decay, $\Delta N = 0, \pm 2$, it was possible to fit the plateaus in CFR to calculated shifts using the theoretical rovibrational energies [52], and so assign certain plateaus to unique rotational levels on a probabilistic basis. Hence, to the extent that the assignment was correct, the uncertainty due to rotational energy was eliminated. Moreover, because the fit averaged over more than 300 runs, a very small statistical uncertainty of 2×10^{-12} was obtained.

As with the alternating technique, in order to correct for the systematic shift due to SR and imbalance in ρ_c, CFR measurements were made with a range of ρ_c in the PnPs. This resulted in a correction of 29.5(1.4) $\times 10^{-12}$. In the simultaneous method, the trap voltage was set so that f_z of the $H_2{}^+$ and D^+ ions were symmetrically below and above the detector resonance frequency. To cool the axial motion before the PnP, each ion was shifted to resonance by changing the trap voltage. This process is necessarily asymmetric, and, because of possible noise spikes or other asymmetries in the detector noise, there was concern that T_z, and so T_c, at the start of the PnPs could be different between the ions,

leading to a systematic SR shift to the CFR. In order to estimate a possible difference in T_c, use was made of the fact that this would also result in a difference in the rms fluctuations in the individual cyclotron frequencies f_{ct1} and f_{ct2}, as discussed above. These frequency fluctuations were determined from the Allan deviation of the long T_{evol} phases of the individual ions. From this, a correction of 2.9(2.9) $\times 10^{-12}$ to the CFR was derived, which was the largest source of systematic uncertainty.

Since f_z did not need to be known precisely, the detector-pushing effect, and in fact all effects that shift the individual f_zs, including ion–ion interaction, had negligible effect on the CFR. Because of the symmetry between the ions, the ion–ion interaction effects on Δf_{ct} and hence the CFR were $<10^{-13}$ and so negligible. There was no $B_1\Delta V$ shift. However, because the ions did not have identical mass, the magnetron radii of the two ions in the coupled magnetron motion were not identical. The resulting correction for trap imperfections and rms magnetron radius difference was $-1.1(0.2) \times 10^{-12}$. Finally, allowing for a possible difference in the rms axial amplitude of the ions due to a difference in T_z during the cyclotron phase evolution, which produces a shift by interacting with B_2, there was a correction of $0.5(0.5) \times 10^{-12}$. The final result for the mass ratio $M[D^+]/M[H_2{}^+(0,0)]$ was 0.999 231 660 003 0(21)(37)(43), (stat)(sys)(total). This result is in excellent agreement with the alternating method. It is also the most precise mass ratio to date. A caveat is that the rotational state identification was probabilistic. If one of the two possible but less probable assignments is chosen, the mass ratio shifts down by 2.7 or 3.6 sigma.

3.4. LIONTRAP Mass of ^{4}He [53]

Following the measurement of the atomic mass of the deuteron, the LIONTRAP apparatus was used by the MPIK collaboration to measure the atomic mass of ^{4}He [53]. Since in LIONTRAP the trap is completely enclosed, a He source was developed that loads gas from a reservoir inside the trap chamber into the creation trap in front of the FEP. Although it was initially planned to measure ^{3}He to help resolve the light-ion puzzle, due to a technical issue only ^{4}He could be loaded, after which it was decided to measure the CFR $^4He^{2+}/^{12}C^{6+}$. This was serendipitous. Their result, using methods that have by now been well validated, was in more than 6-sigma disagreement with the previously accepted result, published by the University of Washington (UW) group nearly 20 years earlier.

As in the measurement of the $D^+/^{12}C^{6+}$ ratio, the ions were trapped in different traps in the electrode stack, each shuttled into the measurement trap for the f_c measurements. The PnA method was used and a CFR measurement consisted of an f_c measurement on each ion, with the first being chosen randomly, the complete CFR measurement taking 3800 s. A single axial detector with resonant frequency near 468 kHz was used, again shifted in frequency using a varactor to match the respective f_{zi} of the two ions at the same trap voltage, eliminating the $B_1\Delta V$ shift. The correction for amplitude-dependent shifts due to SR and trap imperfections was obtained using ρ_c from 10 to 80 μm and fitting the CFR versus the squares of the drive strengths of the respective ions. With a total data set of 482 cycles this gave a CFR with statistical uncertainty of 9×10^{-12}. By using feedback to reduce the ion's axial temperature to 1.7(3) K, the correction and uncertainty due to the ions' cyclotron energy before the cyclotron drive pulse was only $-1.8(0.3) \times 10^{-12}$. Again similar to the $D^+/^{12}C^{6+}$ measurement, the largest systematic correction, at $-65.8(3.3) \times 10^{-12}$, was due to image charge effects, while the largest contribution to the systematic uncertainty, 7.1×10^{-12}, was from the determination of f_z, by fitting the dip in the detector noise signal. Additional corrections due to magnetic field inhomogeneity and electrostatic anharmonicity were essentially negligible. The final result for $3M$ [$^4He^{2+}$]/M [$^{12}C^{6+}$] was 1.000 650 921 192 8(90)(78)(119) (stat), (sys), (total).

3.5. FSU Measurement of $HD^+/^3He^+$, HD^+/T^+ and $T^+/^3He^+$ for the Beta-Decay Q-Value of Tritium and Improved Masses of T and ^{3}He [54]

Previously, in 2014–2015, the FSU group measured the $HD^+/^3He^+$ and HD^+/T^+ CFRs and from the double ratio obtained a Q-value for tritium beta-decay, with an uncertainty

of 0.07 eV [46]. This was the first measurement of light ions by the FSU group and also the start of the so-called light ion (or ^{3}He) mass puzzle. This was the 4-sigma discrepancy between $M[HD^+]/M$ [$^3He^+$] derived from the atomic masses of p, d, and h individually referenced to ^{12}C, and the same mass ratio as measured by FSU. Expressed as a mass difference, $M[p] + M[d] - M[h]$ obtained using $M[d]$ and $M[h]$ from the UW group [55], and $M[p]$ from CODATA-2010 [56] (itself mainly derived from earlier measurements by UW), was greater than that obtained from the FSU $HD^+/^3He^+$ mass ratio [46] by 0.79(18) nu. This was the first indication that some previously accepted values of light ion masses, obtained with single ion Penning trap techniques, might have significantly underestimated uncertainties.

Two years later, using a rebuilt set-up with an improved detector and a more homogeneous magnetic field, and an outer ion radius increased from 1.07 to 2 mm, the FSU group re-measured the $HD^+/^3He^+$ ratio, both directly [2] and also using H_3^+ as an intermediary [47]. This confirmed the original $HD^+/^3He^+$ CFR of [46] and reduced its uncertainty. (The measurements against H_3^+ were complicated by the mass shift due to highly excited, metastable rotational states of H_3^+, and so only produced a lower limit for $2M[p] - M[d]$.) The discrepancy in $M[p] + M[d] - M[h]$ was also partly resolved by the MPIK collaboration's measurements of $M[p]$ [32] and $M[d]$ [45] (see Section 3.2 above). If these replaced the CODATA-2010 [56] and UW [55] values, $M[p] + M[d] - M[h]$ differed from the value from the $HD^+/^3He^+$ ratio of [46] by 0.35(15) nu, and from that of [2] by 0.26(9) nu. Nevertheless, given the remaining discrepancies, and the importance of the tritium Q-value, the FSU group decided to repeat the measurements with tritium using the improved apparatus.

Although the simultaneous method was considered, the measurements used the alternating technique. In the case of $HD^+/^3He^+$ and HD^+/T^+, the ions in the pairs are separated in mass by a fraction of 2×10^{-3}, which resulted in an axial frequency difference of 670 Hz. Consequently, if the trap voltage was set so the ions were positioned symmetrically above and below the detector resonance as required for the simultaneous method, the ions would each be separated by 16 FWHM from the center of the coil resonance, significantly reducing the signal-to-noise for detection of the axial motion. Neither was the simultaneous method applicable to directly measuring $T^+/^3He^+$ since the fractional mass difference is only 6.6×10^{-6}. At the optimum ion–ion separation of 0.8 mm, this would have caused the axial motions of the two ions to be strongly coupled, preventing application of the PnP method. However, with the alternating method, and with the outer ion in a 2 mm radius cyclotron orbit, the separation in f_z between the inner and outer ion was increased to close to 20 Hz due to the residual C_6 and B_2. This enabled PnPs with negligible interference from ion–ion coupling. Compared to using HD^+ as an intermediary, the direct measurement of the $T^+/^3He^+$ CFR reduced the time required to achieve a given statistical uncertainty by a factor of 4. The improved detector compared to [46] enabled the use of a smaller ρ_c, and in combination with a $\times 30$ reduction in B_2, to $-3.7(7) \times 10^{-9}$ mm^{-2}, allowed ρ_c to be varied to quantify the systematic uncertainty due to special relativity and cyclotron radius imbalance. Additionally, with a parking radius of 2 mm, the effects of ion–ion interaction on the CFR were negligible.

Similar to the alternating D^+/H_2^+ measurement, a run typically consisted of 7 h of data taking with 15 interchanges, and yielded a statistical uncertainty of 4×10^{-11} for the best runs. However, this statistical uncertainty was degraded for approximately 50% of the runs due to rapid changes in the ambient magnetic field due to the operation of a magnetic spectrograph in a nearby laboratory, and also due to electromagnetic interference on the detector signal. The final results were based on 84 runs of $HD^+/^3He^+$, 74 of HD^+/T^+ and 79 of $T^+/^3He^+$, with additional runs for calibrating the cyclotron drives and investigating systematic errors. From independent fits to the $HD^+/^3He^+$, HD^+/T^+, and $T^+/^3He^+$ CFRs vs. ${T_d}^2$, non-correlated statistical uncertainties of 11.4, 13.2, and 8.6 $\times 10^{-12}$, respectively, were obtained.

In contrast to the above H_2^+/D^+ measurements, the PnPs were completed at the same f_z. Hence, it could be assumed that the thermal cyclotron energies were balanced,

eliminating any residual relativistic shift after the extrapolation to zero $T_d{}^2$. The detector-pushing effect on f_z between the ions was also balanced, and so had a negligible effect on the CFR. To calibrate the $B_1\Delta V$ shift, measurements were carried out with a $T^+/H_2{}^+$ pair, with the $H_2{}^+$ having been previously stored in a 2 mm cyclotron radius orbit for more than 3 days, so that it could be assumed to be in the $v = 0$ or $v = 1$ vibrational state. Making use of an adequately precise prediction for the $T^+/H_2{}^+$ CFR, a systematic correction of $-1.5(4) \times 10^{-12}$ to be applied to the $HD^+/^3He^+$ and HD^+/T^+ CFRs was determined. A correction of $94.3(1) \times 10^{-12}$ was also applied to these two CFRs to allow for the polarizability of HD^+ [43,44]. All other systematics, including those due to ion–ion interaction were at the level of 10^{-13} or less. After applying the systematic corrections and uncertainties, a least-squares adjustment (LSA) to the three ratios resulted in $M\,[^3He^+]/M[HD^+] = 0.998\,048\,085\,131\,8(92)$, $M[T^+]/M[HD^+] = 0.998\,054\,687\,290\,2(97)$, and $M\,[^3He^+]/M[T^+] = 0.999\,993\,384\,973\,2(77)$, with correlation coefficients (labeling the three ratios as 1,2,3) $r_{12} = 0.67$, $r_{13} = 0.36$, and $r_{23} = -0.46$.

4. Results and Discussion

In this section, the results of the above mass measurements are compared with each other and with other published values of comparable precision.

4.1. M[d], m_d/m_p, and M[p]

4.1.1. M[d]

The deuteron is currently the most precisely measured light ion directly referenced to ^{12}C. In Table 1 $M[d]$ from the LIONTRAP CFR of D^+ against $^{12}C^{6+}$ [45] is compared with the result from CODATA-2018 [1], which is entirely based on the 2015 UW result [55]. As can be seen, the LIONTRAP result is over a factor of two more precise than the CODATA-2018 (UW) result and is lower by 210(43) pu. Also shown is the result of the LSA presented in Table 2 of [45], which incorporates the LIONTRAP $M[p]$ [32], $M[d]$ and $M[HD^+]$ [45], and the 2020 FSU m_d/m_p result of [39]. Also shown is the AME-2020 value [57], which is essentially identical to the LIONTRAP LSA result, the difference being due to the fact that the AME result also includes the $H_3{}^+/HD^+$ result of [47].

Table 1. Results for the atomic mass of the deuteron.

Source	Deuteron Mass (u)
CODATA-2018 (UW 2015) [1,55]	2.013 553 212 745(40)
LIONTRAP 2020 [45]	2.013 553 212 535(17)
LIONTRAP 2020 LSA [45]	2.013 553 212 538(16)
AME-2020 [57]	2.013 553 212 537(15)

4.1.2. m_d/m_p

In Table 2 and Figure 1, we show values for m_d/m_p from CODATA-2018; the result of combining the direct LIONTRAP $M[d]$ (second row of Table 1) with the previously measured LIONTRAP $M[p]$ [32]; and the values for m_d/m_p from the two FSU measurements of $H_2{}^+/D^+$ [39,48]. The two FSU results are in good agreement with each other. This is especially significant given the difference in techniques (alternating cyclotron radii versus couple magnetron orbits) and in the different allowance for rotational energy (from a model versus derived from the CFRs). They also agree with the ratio of the LIONTRAP results. However, it would be inappropriate to combine the FSU results to form a weighted average since the relativistic shift is a common systematic. Additionally, there is a non-negligible chance that the assignment of rotational levels made in [48] should be changed, which could lead to a value for m_d/m_p reduced by up to 32×10^{-12}. The decrease in all the values with respect to CODATA-2018 is consistent with the larger CODATA-2018 (UW 2015) $M[d]$ as shown in Table 1. The recent results are in fair agreement with an earlier measurement of

the H_2^+/D^+ CFR by the SMILETRAP group [58], where neither rotational nor vibrational energy were resolved, which gave m_d/m_p = 1.999 007 500 72(36).

Table 2. Results for m_d/m_p.

Source	m_d/m_p
CODATA-2018 [1]	1.999 007 501 39(11)
LIONTRAP $M[d]/M[p]$ [32,45]	1.999 007 501 223(68)
FSU 2020 [39]	1.999 007 501 274(38)
FSU 2021 [48]	1.999 007 501 272(9)

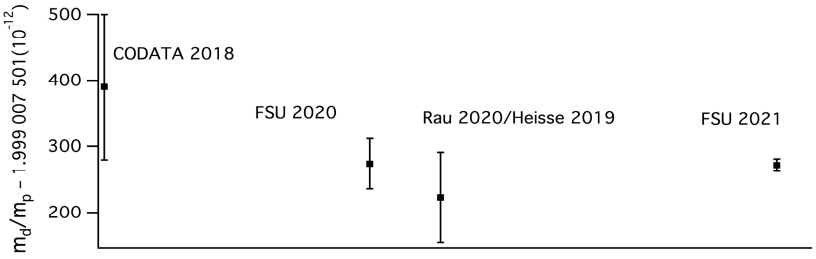

Figure 1. Results for m_d/m_p [1,32,39,45,48]. The data points correspond to Table 2.

4.1.3. M[p]

In Table 3, we show the results for $M[p]$ from CODATA-2018; the direct LIONTRAP measurement against $^{12}C^{6+}$ [32]; the LIONTRAP LSA as in Table 1 above; the AME-2020 result; and the result, at 1×10^{-11} fractional uncertainty, obtained by combining the second FSU value for m_d/m_p [48] with the above LIONTRAP result for $M[d]$ measured directly relative to ^{12}C (second row of Table 1). As can be seen, all these results agree. The CODATA-2018 value represented a compromise between the previously accepted value, mainly based on results from UW [59], and the 2019 LIONTRAP result [32], which was 3-combined-sigma below the UW result. The AME-2020 result is an LSA similar to that executed by the LIONTRAP group in [45], but has a smaller uncertainty by also including results of FSU measurements of H_3^+/HD^+ [47]. The UW results for $M[p]$ and $M[d]$ were not used in the AME-2020 LSA for $M[p]$.

Table 3. Results for $M[p]$.

Source	$M[p]$ (u)
CODATA-2018 [1]	1.007 276 466 621(53)
LIONTRAP [32]	1.007 276 466 598(33)
LIONTRAP LSA [45]	1.007 276 466 580(17)
AME-2020 [57]	1.007 276 466 587(14)
FSU m_d/m_p [48] and LIONTRAP $M[d]$ [45]	1.007 276 466 574(10)

4.2. Q-Value for Tritium Beta Decay, M[p] + M[d] − M[h], and M(h), M(t)

4.2.1. Tritium Beta-Decay Q-Value

The $T^+/^3He^+$ CFR given in Section 3.5 (the result of the LSA of the measured $HD^+/^3He^+$, HD^+/T^+ and $T^+/^3He^+$ CFRs) can be converted into the mass difference between atoms of T and ^{3}He. Expressed in eV/c^2, this gives the Q-value for tritium beta-decay. In Table 4 and Figure 2, this is compared with the previous measurements by the UW [60] and SMILETRAP groups [61], and also the 2015 FSU measurement [46], and the value derived from the "end-point for zero neutrino mass" from the first two data-taking campaigns of the KATRIN

neutrino mass experiment [27]. The two FSU results are 2.2(1.0) eV above the average of the older UW and SMILETRAP results and agree with KATRIN.

Table 4. Tritium beta-decay Q-value (mass difference between neutral atoms) in eV/c^2.

Source	M[T] − M [^{3}He]
UW 1993 [60]	18 590.1(17)
SMILETRAP 2006 [61]	18 589.8(12)
FSU 2015 [46]	18 592.01(7)
KATRIN 2022 [27]	18 591.49(50)
FSU 2023 [54]	18 592.071(22)

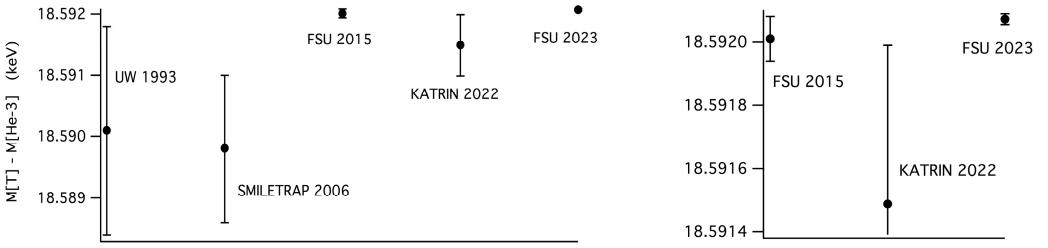

Figure 2. Results for the Tritium Q-value as in Table 4 [27,46,54,60,61]. Left, all results; right, last three results on an expanded scale.

4.2.2. M[p] + M[d] − M[h] and the Light Ion Mass Puzzle

In Table 5 and Figure 3, we compare results for $M[p] + M[d] - M[h]$ obtained from the UW measurements of $M[d]$ and $M[h]$ [55], combined with the CODATA-2010 value for $M[p]$ [56] (mainly derived from UW results); obtained using the LIONTRAP $M[p]$ and $M[d]$ [32,45], but still with UW $M[h]$; the FSU $HD^+/^3He^+$ CFR of [46]; the repeated $HD^+/^3He^+$ measurement with rebuilt apparatus [2]; and the result from the LSA of the recent FSU measurements [54]. (Figure 3 also shows the intermediate result of combining the UW $M[d]$, $M[h]$ [55] and the MPIK $M[p]$ [32]). As can be seen, the three FSU results are in good internal agreement but disagree with results based on masses measured directly against ^{12}C. Specifically, using the latest FSU result as a reference, the UW 2015 plus CODATA-2010 result, and the result using the LIONTRAP $M[p]$ and $M[d]$ but UW $M[h]$, are, respectively, 0.73(11) nu and 0.29(6) nu high. If one assumes that the discrepancies are due to the UW results, this implies that while the UW $M[p]$ and $M[d]$ are too high, the UW $M[h]$ is too low.

Table 5. Results for $M[p] + M[d] - M[h]$.

Source	$M[p] + M[d] - M[h]$ (u)
UW $M[d]$, $M[h]$ [55], CODATA-2010 $M[p]$ [56]	0.005 897 432 889(107)
LIONTRAP $M[p]$, $M[d]$ [32,45]; UW $M[h]$ [55]	0.005 897 432 450(50)
FSU 2015 $HD^+/^3He^+$ [46]	0.005 897 432 097(145)
FSU 2017 $HD^+/^3He^+$ [2]	0.005 897 432 191(70)
FSU 2023 $HD^+/^3He^+$ [54]	0.005 897 432 161(28)

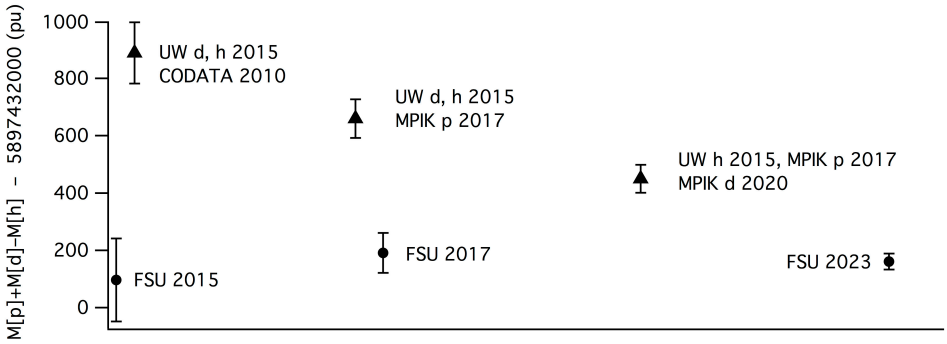

Figure 3. Results for $M[p] + M[d] - M[h]$ as in Table 5 [2,46,54–56], but with the addition of the intermediate result of combining the UW $M[d]$, $M[h]$ [55], and the MPIK $M[p]$ [32].

4.2.3. M[h] and M[t]

Using the (correlated) values for $M[p]$, $M[d]$ from the LSA carried out in [45] results in $M[HD^+]$ of 3.021 378 241 561(26) u, which depends only on LIONTRAP and FSU results. Using this as a reference, the LSA CFRs for $HD^+/^3He^+$ and HD^+/T^+ of [54] then yield values for $M[h]$ and $M[t]$. These are compared with CODATA-2018 and AME-2020 results in Table 6. The AME-2020 result, which is based on the FSU $HD^+/^3He^+$ and HD^+/T^+ CFRs from [46] and the LIONTRAP $M[p]$ and $M[d]$, is in good agreement; the CODATA18 result is similar but is shifted to higher mass since it uses the UW $M[d]$. Otherwise, neither the CODATA18 nor AME2020 use UW data.

Table 6. Results for $M[h]$ and $M[t]$.

Source	$M[h]$ (u)	$M[t]$ (u)
CODATA-2018 [1]	3.014 932 247 175(97)	3.015 500 716 210(120)
AME-2020 [57]	3.014 932 246 960(60)	3.015 500 716 015(81)
FSU 2023 [54]	3.014 932 246 957(38)	3.015 500 716 066(39)

4.3. M[α]

In Table 7, we compare results for the atomic mass of the α-particle from the UW group and the recent LIONTRAP measurement [53]. The UW measurement was originally reported in [62], but was reduced by 22 pu following a re-estimation of the image–charge shift in 2006 [63]. The CODATA-2018 and AME-2020 results are the same as the later UW value, but the AME-2020 value has an uncertainty increased by a factor of 2.5, based on discrepancies for the UW results for $M[d]$ and $M[p]$ with LIONTRAP and FSU results. As can be seen, the UW result is smaller than the LIONTRAP result by more than six combined standard deviations.

Table 7. Results for the mass of the alpha-particle.

Source	M [$^4He^{2+}$] (u)
UW [62]	4.001 506 179 147(64)
CODATA-2018/AME-2020 * [1,57]	4.001 506 179 125(63)
LIONTRAP [53]	4.001 506 179 651(48)

* The uncertainty of the AME2020 value was increased by a factor of 2.5 to 158 pu.

4.4. m_p/m_e and M[e] from HD^+ Spectroscopy Combined with m_d/m_p

As mentioned in the introduction, the remarkable progress in ab initio theory and precision laser and terahertz spectroscopy for rovibrational transitions in HD^+ provide a new route to m_p/m_e and $M[e]$. To lowest order, the rotational and vibrational frequencies of HD^+ are proportional to $R_\infty(m_e/\mu_{p,d})$ and $R_\infty(m_e/\mu_{p,d})^{1/2}$, respectively, where R_∞ is the

Rydberg constant, and $\mu_{p,d} = (1/m_p + 1/m_d)^{-1}$ is the proton–deuteron reduced mass. Since R_∞ can be obtained more accurately from hydrogen spectroscopy, the comparison between theory and experiment for HD^+ can be used to obtain $\mu_{p,d}/m_e$.

From a detailed analysis of experimental and theoretical results for the (v,N)–(v',N') = (0,0)–(0,1), (0,3)–(9,3), and (0,0)–(1,1) transitions, Karr and Koelemeij have obtained $\mu_{p,d}/m_e$ = 1 223.899 228 719(26) [64], which is in good agreement with . . .228 720(25) as obtained by Alighanbari et al. for the recently measured (0,0)–(5,1) transition [13]. Using either of these (the theory uncertainty is dominant and common, so little gain in precision is achieved by averaging), and the value for m_d/m_p of [48] (Table 2), gives the result for m_p/m_e shown in the last row in Table 8. Also shown is the CODATA-2018 value, which is mainly determined using $M[e]$ from the g-factor of $^{12}C^{5+}$ [16], combined with the averaged LIONTRAP and UW result for $M[p]$; and also the result of combining the $^{12}C^{5+}$ g-factor $M[e]$ [1,16] with the updated $M[p]$ in the last row of Table 3. As can be seen, all the results are in reasonable agreement, although there is 1.5-sigma tension between the results obtained from Penning trap measurements only, and that from HD^+ spectroscopy and m_d/m_p.

Table 8. Results for m_p/m_e.

Source	m_p/m_e
CODATA-2018 [1]	1836.152 673 43(11)
$M[e]$ [1,16], updated $M[p]$ (Table 3) [48]	1836.152 673 35(6)
HD^+ spectroscopy [64] + m_d/m_p [48]	1836.152 673 46(4)

Alternatively, the value for $\mu_{p,d}$ from HD^+ spectroscopy [64] can be combined with the FSU result for m_d/m_p [48] and the MPIK $M[d]$ [45] to give $M[e]$. In Table 9, this is compared with $M[e]$ obtained from the g-factor of C^{5+} [1]. Presented this way, the fractional disagreement is 6.2(3.7) $\times$ 10^{-11}.

Table 9. Results for $M[e]$.

Source	$M[e]$
CODATA-2018 (g-factor of C^{5+}) [1,16]	0.548 579 909 065(16) $\times$ 10^{-3}
HD^+ spectroscopy [64] + m_d/m_p [48] + m_d [45]	0.548 579 909 031(13) $\times$ 10^{-3}

5. Conclusions and Outlook

5.1. Partial Resolution of the Light Ion Puzzle, Tritium Q-Value

As the above tables show, since CODATA-2018 there have been significant advances in the determination of masses and mass ratios for all the light ions, with quoted fractional uncertainties now close to or below 1 $\times$ 10^{-11}. There has been some clarification of the discrepancy for $M[p] + M[d] - M[h]$ between FSU and UW results. If the LIONTRAP $M[p]$ and $M[d]$ replace UW values the discrepancy is reduced; also the LIONTRAP results agree with the FSU m_d/m_p. There is also strong disagreement between UW and LIONTRAP for $M[\alpha]$. This suggests that the UW $M[p]$, $M[d]$, and $M[\alpha]$, and so presumably $M[h]$, had underestimated uncertainties. This is likely related to the method used at UW for measuring f_{ct}, which involved applying a frequency-swept modified cyclotron drive and observing the resonant excitation of the cyclotron motion. The cyclotron excitation was detected by monitoring the shift in f_z proportional to ρ_c^2 due to trap imperfections such as B_2. The axial frequency was continually monitored by driving the axial motion with a phase-locked-loop. A study of these methods at MPIK [65] showed that the determination of f_{ct} from fits to the cyclotron resonance line shape, and also the determination of the unperturbed f_z, depended in detail on the parameters of the phase-locked-loop. This resulted in systematic errors at the few $\times 10^{-11}$ level that were difficult to quantify.

Nevertheless, a measurement of $M[h]$ by MPIK or another group is motivated to confirm the FSU measurements. Likewise, an additional, independent measurement of $M[\alpha]$ is strongly motivated, especially since $M[\alpha]$ is required for obtaining $M[e]$ using the g-factor of He^+. Although the consistency between the FSU $T^+/^3He^+$ CFR obtained directly and by using HD^+ as an intermediary, and between the 2015 and 2023 results (the latter being analyzed blind with respect to the former) are compelling, given the importance of the absolute neutrino mass experiments, there is still a case for measurements on tritium by another group.

5.2. Interplay of Penning Trap Mass Measurements, g-Factor Measurements, Molecular Hydrogen Ion Spectroscopy, and Electron Atomic Mass

Table 9 shows only a modest improvement in precision for $M[e]$ from combining the new light-ion masses with the results of HD^+ spectroscopy. This is due to uncertainty in the QED theory for the (hyperfine-averaged) rovibrational transitions, and due to discrepancies between individual hyperfine components and hyperfine theory [64]. However, some of the measured hyperfine components of the HD^+ vibrational transitions have quoted uncertainties as small as 1.5×10^{-12}. In principle, if the hyperfine discrepancies can be resolved, and the uncertainty in the QED theory for the rovibrational transitions reduced, HD^+ spectroscopy and the current Penning trap m_d/m_p could result in m_p/m_e with a fractional uncertainty of only 3×10^{-12}, an order of magnitude improvement over CODATA-2018. Conversely, a factor of 10 improved Penning trap $\mu_{p,d}/m_e$ would permit a test of the QED theory for HD^+, and a search for beyond-standard-model physics at the few ppt level. The situation will become even more interesting when precision spectroscopic measurements of rovibrational transitions in H_2^+, D_2^+, and possibly T_2^+ become available, since these will yield m_p/m_e, m_d/m_e, and m_t/m_e more directly. As discussed in [66], a rigorous treatment of all the experimental results requires an LSA in which theoretical uncertainties in the QED theory and perturbations due to beyond-standard-model interactions are treated in a consistent way. In any case, Penning trap measurements of $M[p]$, $M[d]$, and $M[t]$ and their ratios, and also g-factor measurements for $M[e]$, with sub-10^{-11} fractional uncertainty, are motivated.

5.3. Future Developments

Observing that the LIONTRAP and FSU methods have much in common, single-ion cryogenic Penning trap techniques appear to have reached a level of maturity. In the case of the FSU work, the main limitations to precision are still variations in the magnetic field (except when the simultaneous method can be applied), detector noise, and, for light ions, noise on the cyclotron frequency due to fluctuations on the cyclotron radius and special relativity. Although in principle these issues all have technical solutions, e.g., improved magnetic shielding, the use of feedback and the PnA method, the goal of a mass ratio at 1×10^{-12} is still elusive.

It is possible to extend the coupled-magnetron-orbit, simultaneous method to poorer mass-doublets. This can be achieved by applying modulation to the ring-voltage to create sidebands on the axial motion close to the detector resonance. Alternatively, detectors resonant at two axial frequencies could be used. If the ions can be cooled to sub-kelvin temperatures, e.g., with a dilution refrigerator [20] or by sympathetic laser cooling [67], the SR noise and systematic SR shifts could be greatly reduced, but at the cost of greater experimental complexity. In the case of LIONTRAP, SR is somewhat less of an issue due to the lower magnetic field. The uncertainty due to measurement of the axial frequency could be reduced, e.g., using a phase-sensitive method, or working off-resonance to narrow the axial resonance. Perhaps surprisingly, the method of simultaneously measuring f_c of an ion pair with the two ions in adjacent precision traps, and then swapping them, or using a third ion as a reference [29,31,68,69] has not yet resulted in improved CFR measurements. This technique, combined with colder ions and more sensitive detection methods, could lead to a significant improvement in precision.

For a new m_d/m_p using H_2^+/D^+, it would be possible to achieve rovibrational state identification by combining a precision mass measurement trap with a trap used for g-factor measurement [23]. This could also be applied to CFRs involving D_2^+, e.g., for $D_2^+/^4He^+$, and even T_2^+. There are also opportunities to provide additional cross-checks on light ion masses using mass doublets such as $DH_2^+/^4He^+$ and $TH^+/^4He^+$. Here, since electric-dipole transitions are allowed due to the lack of molecular symmetry, the molecular ions can be assumed to be in the rovibrational ground state.

Funding: This research was funded by the U.S. National Science Foundation under award number 1912095.

Data Availability Statement: This article is a review based on the literature and presents no original data.

Acknowledgments: The author thanks Moisés Medina Restrepo for reading the manuscript.

Conflicts of Interest: The author declares no conflict of interest.

References

1. Tiesinga, E.; Mohr, P.J.; Newell, D.B. CODATA recommended values of the fundamental physical constants: 2018. *J. Phys. Chem. Ref. Data* **2021**, *50*, 033105. [CrossRef]
2. Hamzeloui, S.; Smith, J.A.; Fink, D.J.; Myers, E.G. Precision mass ratio of $^3He^+$ to HD^+. *Phys. Rev. A* **2017**, *96*, 060501. [CrossRef]
3. Myers, E.G. High-precision atomic mass measurements for fundamental constants. *Atoms* **2019**, *7*, 3. [CrossRef]
4. Korobov, V.I.; Hilico, L.; Karr, J.-P. Fundamental transitions and ionization energies of the hydrogen molecular ions with few ppt uncertainty. *Phys. Rev. Lett.* **2017**, *118*, 233001. [CrossRef] [PubMed]
5. Aznabayev, D.T.; Bekbaev, A.K.; Korobov, V.I. Leading-order relativistic corrections to the rovibrational spectrum of H_2^+ and HD^+ molecular ions. *Phys. Rev. A* **2019**, *99*, 012501. [CrossRef]
6. Korobov, V.I.; Karr, J.-P. Rovibrational spin-averaged transitions in the hydrogen molecular ions. *Phys. Rev. A* **2021**, *104*, 032806. [CrossRef]
7. Schmidt, J.; Louvradoux, T.; Heinrich, J.; Sillitoe, N.; Simpson, M.; Karr, J.-P.; Hilico, L. Trapping, Cooling, and photodisociation analysis of state-selected H_2^+ ions produced by (3+1) multiphoton ionization. *Phys. Rev. Appl.* **2020**, *14*, 024053. [CrossRef]
8. Schwegler, N.; Holzapfel, D.; Stadler, M.; Mitjans, A.; Sergachev, I.; Home, J.P.; Kienzler, D. Trapping and ground-state cooling of a single H_2^+. *Phys. Rev. Lett.* **2023**, *131*, 133003. [CrossRef]
9. Schiller, S.; (H. H. Universität, Düsseldorf, Germany). Personal communication, 2023.
10. Alighanbari, S.; Giri, G.S.; Constantin, F.L.; Korobov, V.I.; Schiller, S. Precise tests of quantum electrodynamics and determination of fundamental constants with HD^+ ions. *Nature* **2020**, *581*, 152. [CrossRef]
11. Patra, S.; Germann, M.; Karr, J.-P.; Haidar, M.; Hilico, L.; Korobov, V.I.; Cozijn, F.M.J.; Eikema, K.S.E.; Ubachs, W.; Koelemeij, J.C.J. Proton-electron mass ratio from laser spectroscopy of HD^+ at the part-per-trillion level. *Science* **2020**, *369*, 1238. [CrossRef]
12. Kortunov, I.V.; Alighanbari, S.; Hansen, M.G.; Giri, G.S.; Korobov, V.I.; Schiller, S. Proton-electron mass ratio by high-resolution optical spectroscopy of ion ensembles in the resolved carrier regime. *Nat. Phys.* **2021**, *17*, 569. [CrossRef]
13. Alighanbari, S.; Kortunov, I.V.; Giri, G.S.; Schiller, S. Test of charged baryon interactions with high-resolution spectroscopy of molecular hydrogen ions. *Nat. Phys.* **2023**, *19*, 1263.
14. Germann, M.; Patra, S.; Karr, J.-P.; Hilico, L.; Korobov, V.I.; Salumbides, E.J.; Eikema, K.S.E.; Ubachs, W.; Koelemeij, J.C.J. Three-body QED test and fifth-force constraint from vibrations and rotations of HD^+. *Phys. Rev. Res.* **2021**, *3*, L022028. [CrossRef]
15. Czarnecki, A.; Dowling, M.; Piclum, J.; Szafron, R. Two-loop binding corrections to the electron gyromagnetic factor. *Phys. Rev. Lett.* **2018**, *120*, 043203. [CrossRef] [PubMed]
16. Zatorski, J.; Sikora, B.; Karshenboim, S.G.; Sturm, S.; Köhler-Langes, F.; Blaum, K.; Keitel, C.H.; Harman, Z. Extraction of the electron mass from g-factor measurements on light hydrogenlike ions. *Phys. Rev. A* **2017**, *96*, 012502. [CrossRef]
17. Sturm, S.; Köhler, F.; Zatorski, J.; Wagner, A.; Harmann, Z.; Werth, G.; Quint, W.; Keitel, C.H.; Blaum, K. High precision measurement of the atomic mass of the electron. *Nature* **2014**, *506*, 467. [CrossRef] [PubMed]
18. Köhler, F.; Sturm, S.; Kracke, A.; Werth, G.; Quint, Q.; Blaum, K. The electron mass from g-factor measurements on hydrogen-like carbon $^{12}C^{5+}$. *J. Phys. B At. Mol. Opt. Phys.* **2015**, *48*, 144032. [CrossRef]
19. Farnham, D.L.; Van Dyck, R.S.; Schwinberg, P.B. Determination of the electron's atomic mass and the proton/electron mass ratio via Penning trap mass spectroscopy. *Phys. Rev. Lett.* **1995**, *75*, 3598. [CrossRef]
20. Fan, X.; Myers, T.G.; Sukra, B.A.D.; Gabrielse, G. Measurement of the Electron Magnetic Moment. *Phys. Rev. Lett.* **2023**, *130*, 071801. [CrossRef]
21. Brown, L.S.; Gabrielse, G. Geonium theory: Physics of a single electron or ion in a Penning trap. *Rev. Mod. Phys.* **1986**, *58*, 233. [CrossRef]
22. Schneider, A.; Sikora, B.; Dickopf, S.; Müller, M.; Oreshkina, N.S.; Rischka, A.; Valuev, I.A.; Ulmer, S.; Walz, J.; Harman, Z.; et al. Direct measurement of the 3He+ magnetic moments. *Nature* **2022**, *606*, 878. [CrossRef]
23. Myers, E.G. CPT tests with the antihydrogen molecular ion. *Phys. Rev. A* **2018**, *98*, 010101. [CrossRef]
24. König, C.; (MPIK, Heidelberg, Germany). Personal communication, 2023.

25. Karr, J.-P. Leading-order relativistic corrections to the g-factor of H_2^+. *Phys. Rev. A* **2021**, *104*, 032822. [CrossRef]
26. Workman, R.L.; Burkert, V.D.; Crede, V.; Klempt, E.; Thoma, U.; Tiator, L.; Agashe, K.; Aielli, G.; Allanach, B.C.; Amsler, C.; et al. The review of particle physics 2022. *Prog. Theor. Exp. Phys.* **2022**, *8*, 083C01.
27. The KATRIN Collaboration. Direct neutrino-mass measurement with sub-electron volt sensitivity. *Nat. Phys.* **2022**, *18*, 160–166. [CrossRef]
28. Esfahani, A.A.; Böser, S.; Buzinsky, N.; Carmona-Benitez, M.C.; Claessens, C.; De Viveiros, L.; Doe, P.J.; Fertl, M.; Formaggio, J.A.; Gaison, J.K.; et al. Tritium beta spectrum and neutrino mass limit from cyclotron radiation emission spectroscopy. *Phys. Rev. Lett.* **2023**, *131*, 102502. [CrossRef]
29. Myers, E.G. The most precise atomic mass measurements in Penning traps. *Int. J. Mass Spectrom.* **2013**, *349–350*, 107. [CrossRef]
30. Vogel, M. *Particle Confinement in Penning Traps*; Springer: Cham, Switzerland, 2018.
31. Thompson, J.K. Two-ion control and polarization forces for precise mass comparisons. Ph.D. Thesis, Massachusetts Institute of Technology, Cambridge, MA, USA, 2003.
32. Heisse, F.; Rau, S.; Köhler-Langes, F.; Quint, W.; Werth, G.; Sturm, S.; Blaum, K. High-precision mass spectrometer for light ions. *Phys. Rev. A* **2019**, *100*, 022518. [CrossRef]
33. Borchert, M.J.; Devlin, J.A.; Erlewein, S.R.; Fleck, M.; Harrington, J.A.; Higuchi, T.; Latacz, B.M.; Voelksen, F.; Wursten, E.J.; Abbass, F.; et al. A 16-parts-per-trillion measurement of the antiproton-to-proton charge-mass ratio. *Nature* **2022**, *601*, 53. [CrossRef]
34. Cornell, E.A.; Weisskoff, R.M.; Boyce, K.R.; Pritchard, D.E. Mode coupling in a Penning trap: Pi pulses and a classical avoided crossing. *Phys. Rev. A* **1990**, *41*, 112. [CrossRef]
35. Cornell, E.A.; Weisskoff, R.M.; Boyce, K.R.; Flanagan, R.W.; Lafyatis, G.P.; Pritchard, D.E. Single-ion cyclotron resonance measurement of $M(CO^+)/M(N_2^+)$. *Phys. Rev. Lett.* **1989**, *63*, 1674. [CrossRef] [PubMed]
36. Redshaw, M.; McDaniel, J.; Shi, W.; Myers, E.G. Mass ratio of two ions in a Penning trap by alternating between the trap center and a large cyclotron orbit. *Int. J. Mass Spectrom.* **2006**, *251*, 125. [CrossRef]
37. Gabrielse, G.; Haarsma, L.; Rolston, S.L. Open-endcap Penning traps for high precision experiments. *Int. J. Mass Spectrom. Ion Process.* **1989**, *88*, 319. [CrossRef]
38. Sturm, S.; Wagner, A.; Schabinger, B.; Blaum, K. Phase sensitive cyclotron frequency measurements at ultralow energies. *Phys. Rev. Lett.* **2011**, *107*, 143003. [CrossRef] [PubMed]
39. Fink, D.J.; Myers, E.G. Deuteron to proton mass ratio from the cyclotron frequency ratio of H_2^+ to D^+ with H_2^+ in a resolved vibrational state. *Phys. Rev. Lett.* **2020**, *124*, 013001. [CrossRef] [PubMed]
40. Von Busch, F.; Dunn, G.H. Photodissociation of H_2^+ and D_2^+: Experiment. *Phys. Rev. A* **1972**, *5*, 1726. [CrossRef]
41. Posen, A.G.; Dalgarno, A.; Peek, J.M. The quadrupole vibration-rotation transition probabilities of the molecular hydrogen ion. *At. Data Nucl. Data Tables* **1983**, *28*, 265–277. [CrossRef]
42. Karr, J.-P. Stark quenching of rovibrational states of H_2^+ due to motion in a magnetic field. *Phys. Rev. A* **2018**, *98*, 062501. [CrossRef]
43. Cheng, M.; Brown, J.M.; Rosmus, P.; Linguerri, R.; Komiha, N.; Myers, E.G. Dipole moments and orientation polarizabilities of diatomic molecular ions for precision atomic mass measurements. *Phys. Rev. A* **2007**, *75*, 012502. [CrossRef]
44. Schiller, S.; Bakalov, D.; Bekbaev, A.K.; Korobov, V.I. Static and dynamic polarizability and the Stark and black-body-radiation frequency shifts of the molecular hydrogen ions H_2^+, HD^+, and D_2^+. *Phys. Rev. A* **2014**, *89*, 052521. [CrossRef]
45. Rau, S.; Heisse, F.; Köhler-Langes, F.; Sasidharan, S.; Haas, R.; Renisch, D.; Düllman, C.E.; Quint, W.; Sturm, S.; Blaum, K. Penning trap mass measurement of the deuteron and HD^+ molecular ion. *Nature* **2020**, *585*, 43. [CrossRef]
46. Myers, E.G.; Wagner, A.; Kracke, H.; Wesson, B.A. Atomic masses of tritium and helium-3. *Phys. Rev. Lett.* **2015**, *114*, 013003. [CrossRef] [PubMed]
47. Smith, J.A.; Hamzeloui, S.; Fink, D.J.; Myers, E.G. Rotational energy as mass in H_3^+ and lower limits on the atomic masses of D and ^{3}He. *Phys. Rev. Lett.* **2018**, *120*, 143002. [CrossRef] [PubMed]
48. Fink, D.J.; Myers, E.G. Deuteron to proton mass ratio from simultaneous measurement of the cyclotron frequencies of H_2^+ to D^+. *Phys. Rev. Lett.* **2021**, *127*, 243001. [CrossRef] [PubMed]
49. Cornell, E.A.; Boyce, K.R.; Fygenson, D.L.K.; Pritchard, D.E. Two ions in a Penning trap: Implications for precision mass spectroscopy. *Phys. Rev. A* **1992**, *45*, 3049. [CrossRef]
50. Rainville, S.; Thompson, J.K.; Pritchard, D.E. An ion balance for ultra-high precision atomic mass measurements. *Science* **2004**, *303*, 334. [CrossRef] [PubMed]
51. D'Urso, B.; Odom, B.; Gabrielse, G. Feedback cooling of a one-electron oscillator. *Phys. Rev. Lett.* **2003**, *90*, 043001. [CrossRef] [PubMed]
52. Moss, R.E. Calculations for the vibration-rotation levels of H_2^+ in its ground and first excited electronic states. *Mol. Phys.* **1993**, *80*, 1541. [CrossRef]
53. Sasidharan, S.; Bezrodnova, O.; Rau, S.; Quint, W.; Sturm, S.; Blaum, K. Penning-trap mass measurement of helium-4. *Phys Rev. Lett.* **2023**, *131*, 093201. [CrossRef]
54. Medina Restrepo, M.; Myers, E.G. Mass difference of tritium and helium-3. *Phys. Rev. Lett.* **2021**, *127*, 243001. [CrossRef]
55. Zafonte, S.L.; Van Dyck, R.S., Jr. Ultra-precise single-ion atomic mass measurements on deuterium and helium-3. *Metrologia* **2015**, *52*, 280. [CrossRef]

56. Mohr, P.J.; Taylor, B.N.; Newell, D.B. CODATA recommended values of the fundamental physical constants: 2010. *Rev. Mod. Phys.* **2012**, *84*, 1527. [CrossRef]
57. Wang, M.; Huang, W.J.; Kondev, F.G.; Audi, G.; Naimi, S. The AME 2020 atomic mass evaluation (II). Tables, graphs, and references. *Chin. Phys. C* **2021**, *45*, 030003. [CrossRef]
58. Solders, A.; Bergström, I.; Nagy, S.; Suhonen, M.; Schuch, R. Determination of the proton mass from a measurement of the cyclotron frequencies of D^+ to H_2^+ in a Penning trap. *Phys. Rev. A* **2008**, *78*, 012514. [CrossRef]
59. Van Dyck, R.S.; Farnham, D.L.; Zafonte, S.L.; Schwinberg, P.B. High precision Penning trap mass spectroscopy and a new measurement of the proton's atomic mass. *AIP Conf. Proc.* **1999**, *457*, 101.
60. Van Dyck, R.S.; Farnham, D.L.; Schwinberg, P.B. Tritium-helium-3 mass difference using the Penning trap mass spectroscopy. *Phys. Rev. Lett.* **1993**, *70*, 2888. [CrossRef] [PubMed]
61. Nagy, S.; Fritioff, T.; Björkhage, M.; Bergström, I.; Schuch, R. On the *Q*-value of the tritium beta-decay. *Europhys. Lett.* **2006**, *74*, 404. [CrossRef]
62. Van Dyck, R.S.; Zafonte, S.L.; Van Liew, S.; Schwinberg, P.B. Ultraprecise atomic mass measurement of the alpha particle and ^{4}He. *Phys. Rev. Lett.* **2004**, *92*, 220802. [CrossRef]
63. Van Dyck, R.S.; Pinegar, D.B.; Van Liew, S.; Zafonte, S.L. The UW-PTMS: Systematic studies, measurement progress, and future developments. *Int. J. Mass Spectrom.* **2006**, *251*, 231. [CrossRef]
64. Karr, J.-P.; Koelemeij, J.C.J. Extraction of spin-averaged rovibrational transition frequencies in HD^+ for the determination of fundamental constants. *Mol. Phys.* **2023**, *121*, e2215081. [CrossRef]
65. Höcker, M.J. Precision Mass Measurements at The-Trap and the FSU Trap. Ph.D. Thesis, University of Heidelberg, Heidelberg, Germany, 2016.
66. Delaunay, C.; Karr, J.-P.; Kitahara, T.; Koelemeij, J.C.J.; Soreq, Y.; Zupan, J. Self-consistent extraction of spectroscopic bounds on light new physics. *Phys. Rev. Lett.* **2023**, *130*, 121801. [CrossRef]
67. Will, C.; Bohman, M.; Driscoll, T.; Wiesinger, M.; Abbass, F.; Borchert, M.J.; A Devlin, J.; Erlewein, S.; Fleck, M.; Latacz, B.; et al. Sympathetic cooling schemes for separately trapped ions coupled via image currents. *New J. Phys.* **2022**, *24*, 033021. [CrossRef]
68. Repp, J.; Böhm, C.; López-Urrutia, J.R.C.; Dörr, A.; Eliseev, S.; George, S.; Goncharov, M.; Novikov, Y.N.; Roux, C.; Sturm, S.; et al. PENTATRAP: A novel cryogenic multi-Penning-trap experiment for high-precision mass measurements on highly charged ions. *Appl. Phys. B* **2012**, *107*, 983. [CrossRef]
69. Redshaw, M.; Bhandari, R.; Gamage, N.; Hasan, M.; Horana Gamage, M.; Keblbeck, D.K.; Limarenko, S.; Perera, D. Status of CHIP-TRAP: The central Michigan University high-precision Penning trap. *Atoms* **2023**, *11*, 127. [CrossRef]